

Supplementary Information

Parallel shRNA and CRISPR-Cas9 screens enable antiviral drug target identification

Richard M. Deans^{1,2}, David W. Morgens², Ayşe Ökesli¹, Sirika Pillay³, Max A. Horlbeck⁴, Martin Kampmann⁴, Luke A. Gilbert⁴, Amy Li², Roberto Mateo³, Mark Smith⁵, Jeffrey S. Glenn^{3,5,6}, Jan E. Carette³, Chaitan Khosla^{1,5,7,8*},
and Michael C. Bassik^{2,5*}

Affiliations:

¹Department of Chemistry, Stanford University, Stanford, CA 94305, USA

²Department of Genetics, Stanford University, Stanford, CA 94305, USA

³Department of Microbiology and Immunology, Stanford University, Stanford, CA 94305, USA

⁴Department of Cellular and Molecular Pharmacology, California Institute for Quantitative Biomedical Research and Howard Hughes Medical Institute, San Francisco, CA 94158, USA

⁵Stanford University Chemistry, Engineering, and Medicine for Human Health (ChEM-H), Stanford, CA 94305, USA

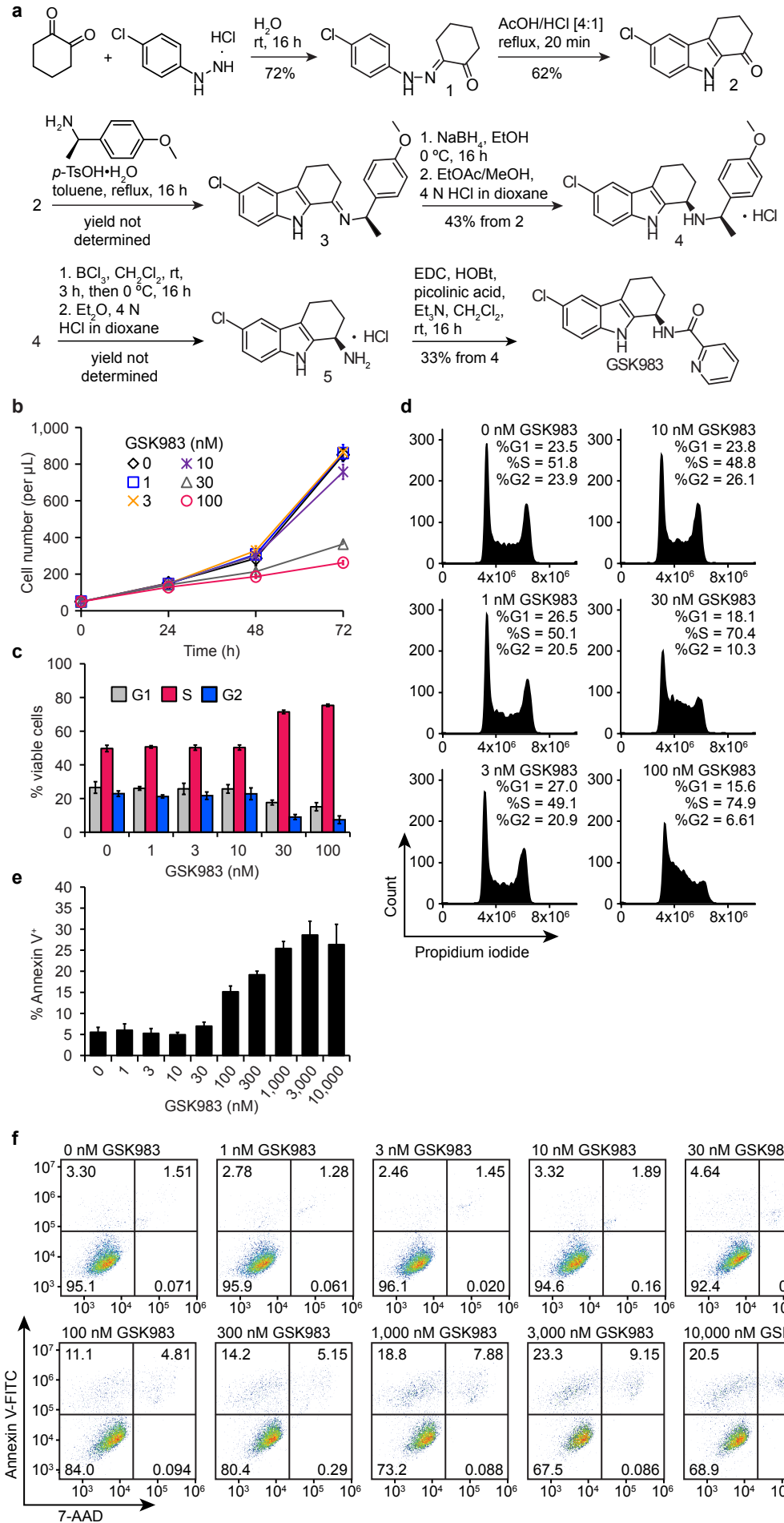
⁶Stanford University School of Medicine, Division of Gastroenterology and Hepatology, Stanford, CA 94305, USA

⁷Department of Chemical Engineering, Stanford University, Stanford, CA 94305, USA

⁸Department of Biochemistry (by courtesy), Stanford University, Stanford, CA 94305, USA

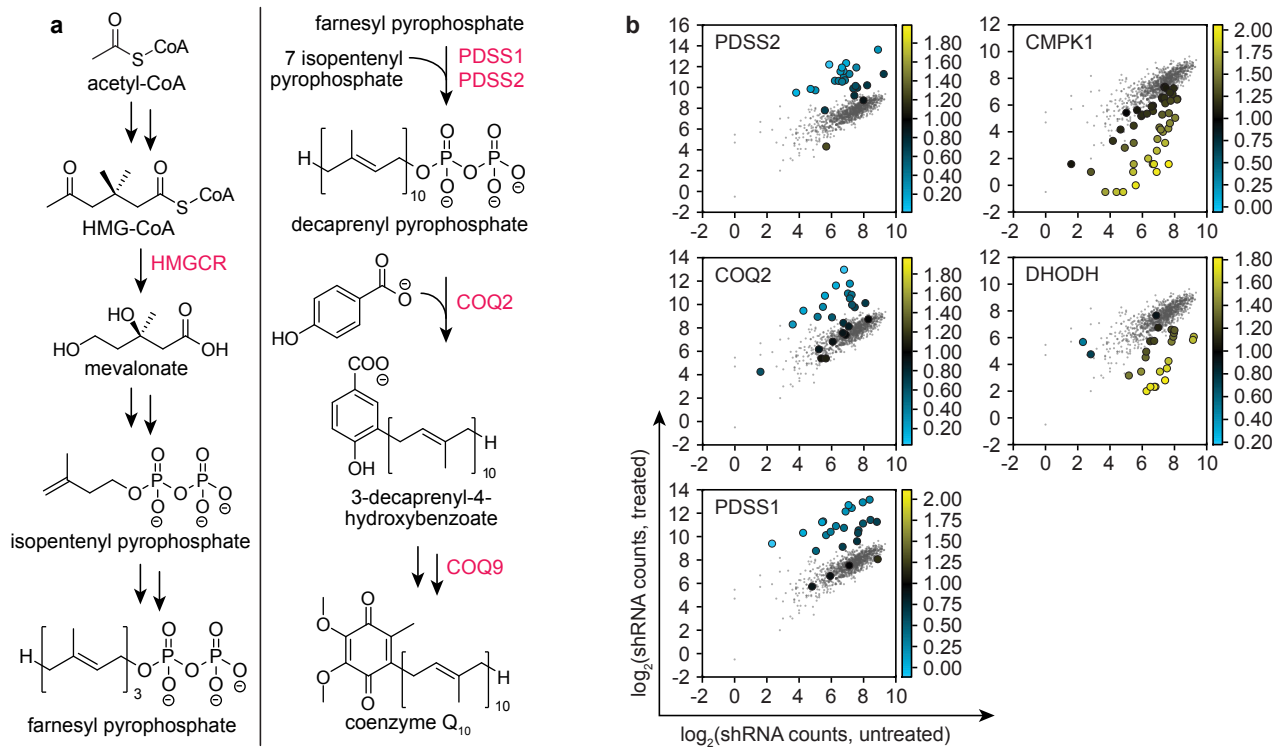
*Correspondence to: bassik@stanford.edu, khosla@stanford.edu

Supplementary Figure 1



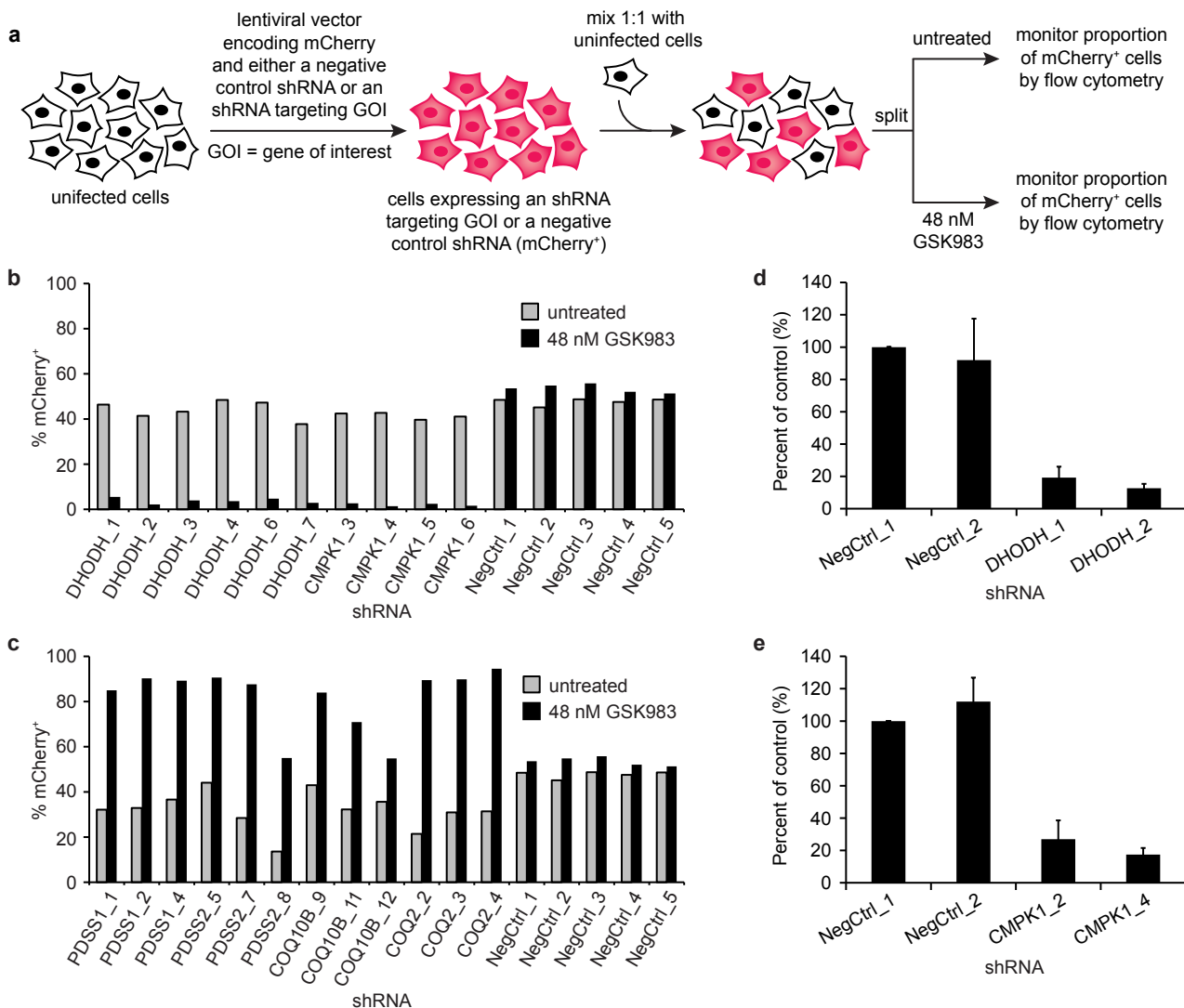
Supplementary Figure 1. (a) Synthesis of GSK983. (b) Time-dependence of GSK983-induced growth inhibition in K562 cells. Viable cells were counted by flow cytometry (FSC/SSC) at the indicated time points following treatment with 0–100 nM GSK983. Error bars represent \pm standard deviation of 4 biological replicates. (c) GSK983-induced S phase cell cycle arrest in K562 cells. Cells were treated with the indicated concentration of GSK983 for 24 h, fixed in 70% EtOH, stained with propidium iodide, and analyzed by flow cytometry. (d) Cell cycle analysis of GSK983-treated K562 cells. Flow cytometry plots depict one of three biological replicates from data summarized in Supplementary Fig. 1c. (e) GSK983-induced apoptosis in K562 cells. Cells were treated with the indicated concentration of GSK983 for 72, fixed in 70% EtOH, stained with annexin V-FITC and 7-AAD, and analyzed by flow cytometry. Error bars represent \pm standard deviation of 4 biological replicates. (f) GSK983-induced apoptosis in K562 cells. Flow cytometry plots depict one of four biological replicates from data summarized in Supplementary Fig. 1e.

Supplementary Figure 2



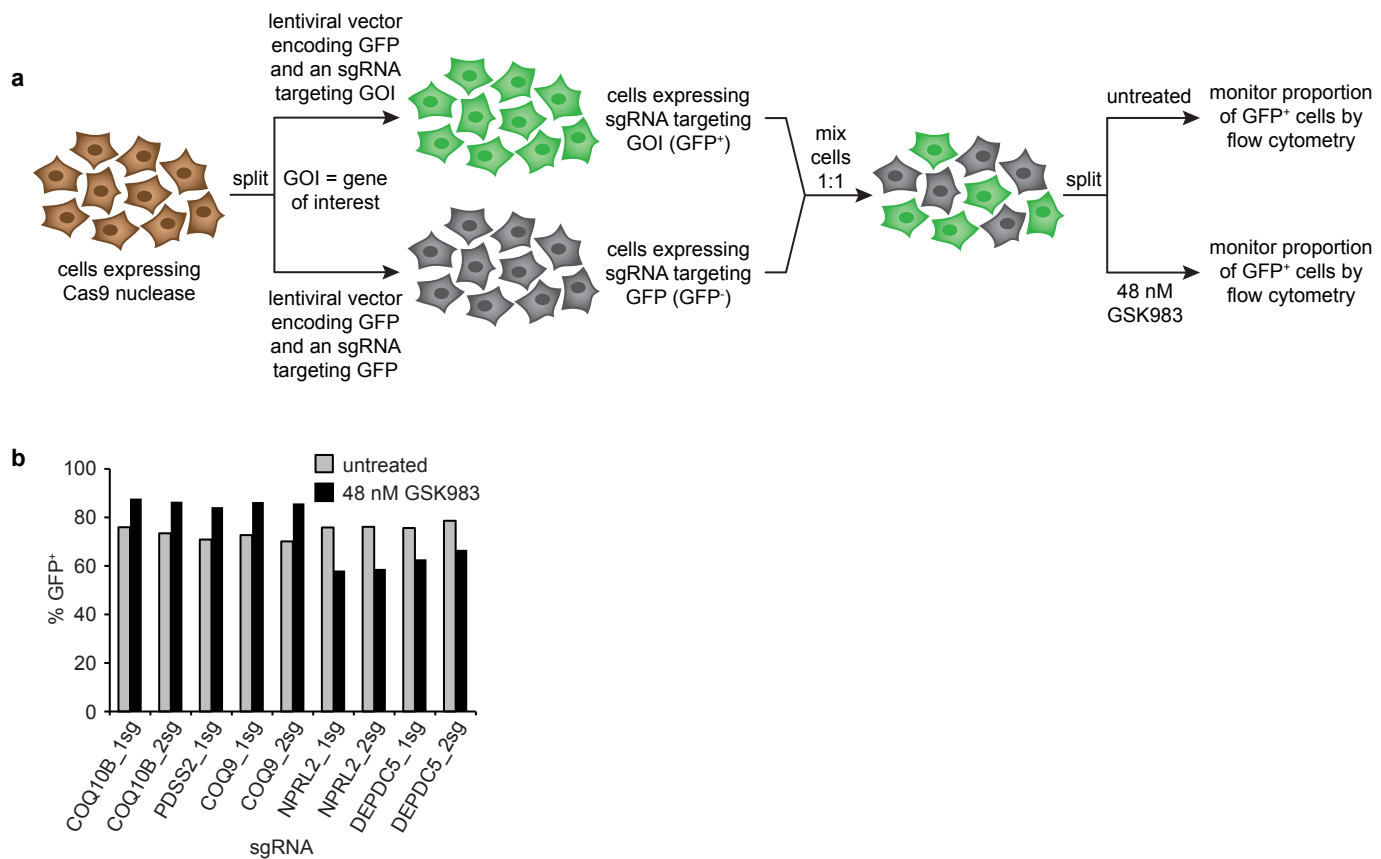
Supplementary Figure 2. (a) Mammalian coenzyme Q₁₀ (CoQ₁₀) biosynthesis. Genes shown in bold appeared among the top ten hits in the shRNA screen (PDSS2, COQ2, PDSS1) and/or CRISPR-Cas9 screen (PDSS2, COQ9, HMGCR, PDSS1). (b) Comparison of counts of shRNA-encoding constructs in genomic DNA isolated from untreated and GSK983-treated cells following our genome-wide shRNA screen. For each plot, the enlarged, colored circles represent shRNAs targeting the indicated gene. The grey cloud represents the set of negative control shRNAs.

Supplementary Figure 3



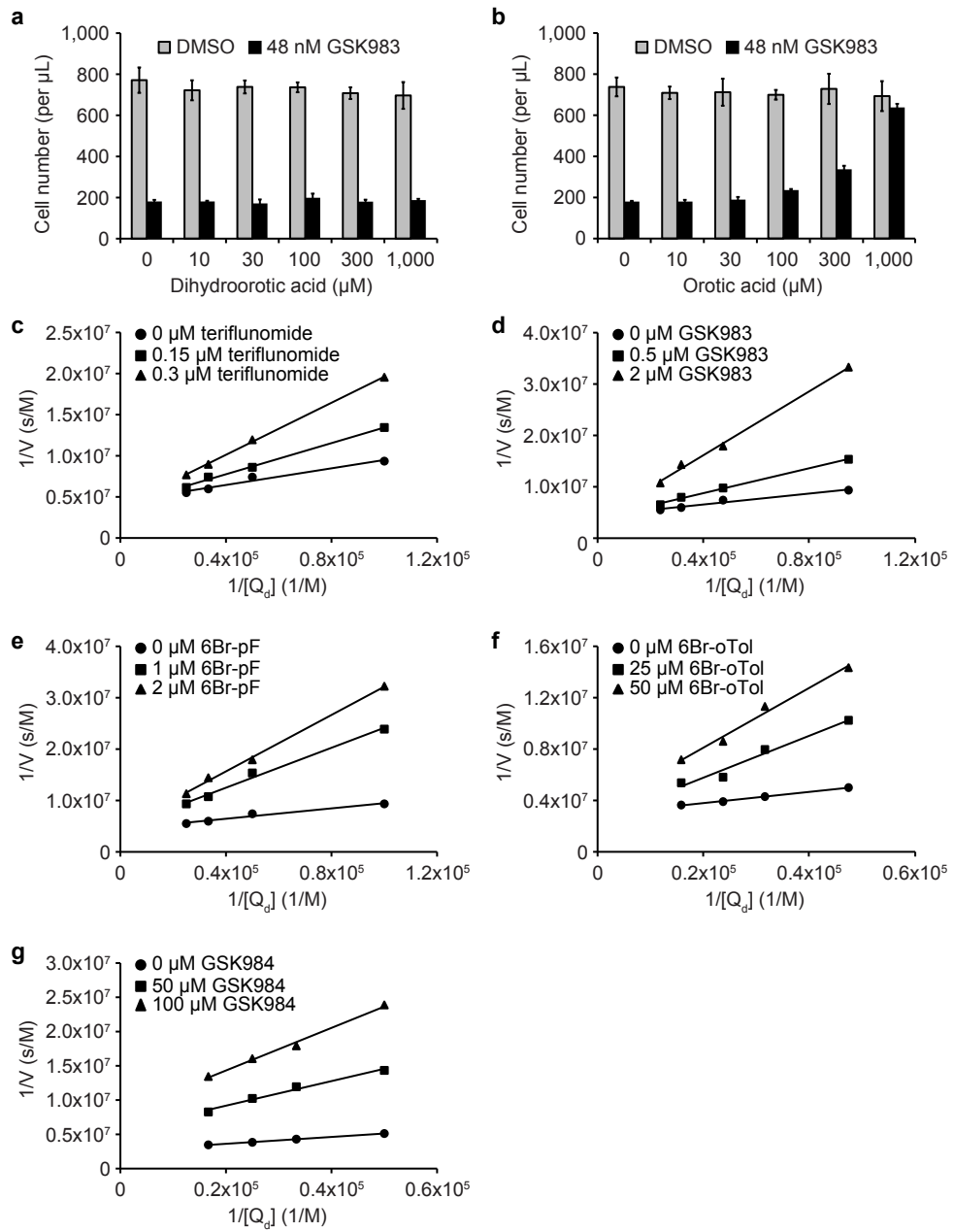
Supplementary Figure 3. (a) Schematic representation of competitive growth assays used to retest individual shRNAs. (b) shRNA-mediated knockdown of DHODH or CMPK1 sensitized K562 cells to GSK983 in competitive growth assays. Six shRNAs targeting DHODH, four shRNAs targeting CMPK1, and five negative control shRNAs were retested. Bars represent the average of two biological replicates. (c) shRNA-mediated knockdown of PDSS1, PDSS2, COQ10B, and COQ2 protected K562 cells against GSK983 in competitive growth assays. Three shRNAs targeting each gene and five negative control shRNAs were retested. Bars represent the average of two biological replicates. qPCR to confirm the efficacy of selected shRNAs targeting DHODH (d), and CMPK1 (e). Measurements are the average of 3 replicates, error bars represent \pm standard deviation of 3 biological replicates. All values are normalized to the first of two negative control shRNAs.

Supplementary Figure 4



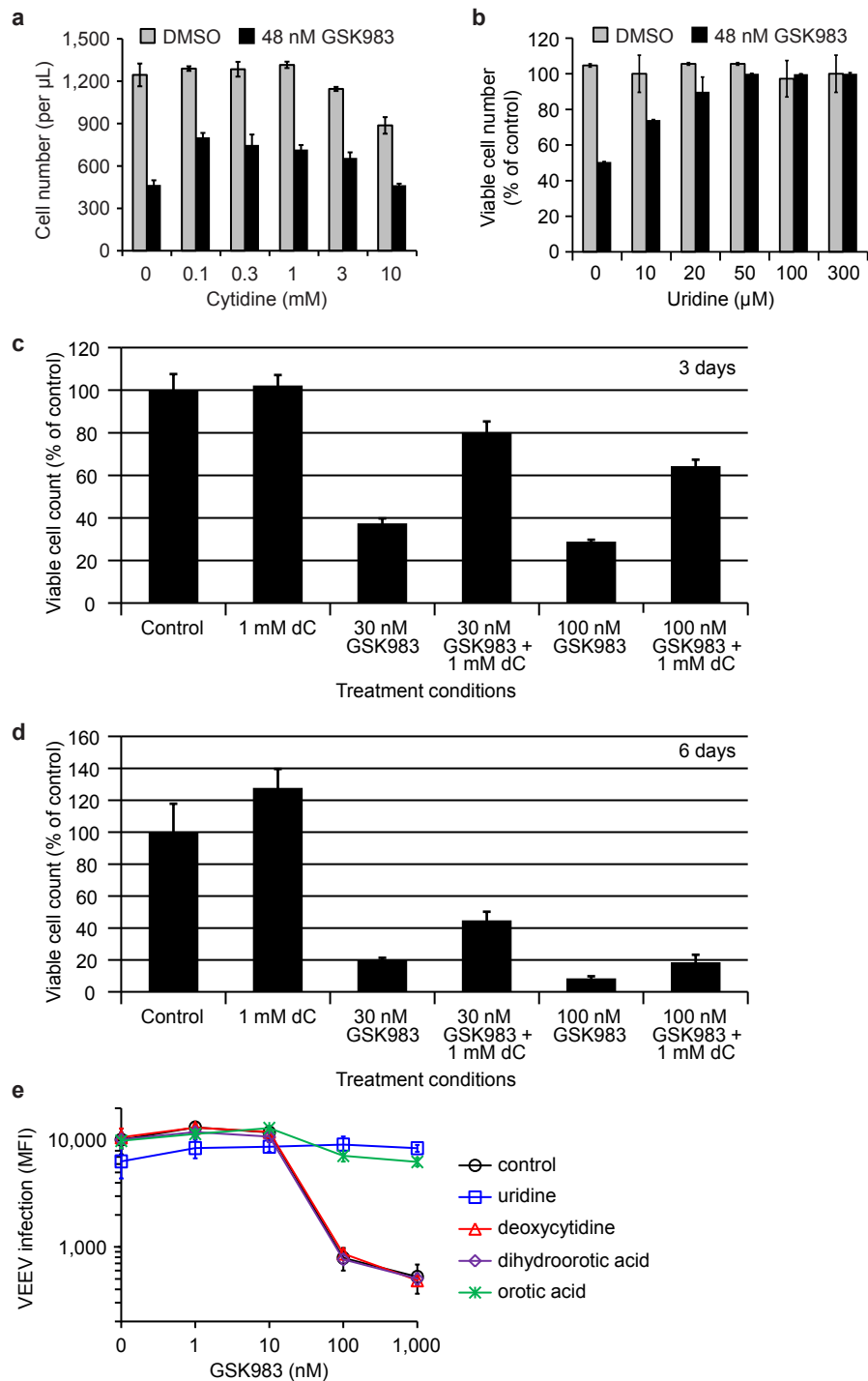
Supplementary Figure 4. (a) Schematic representation of competitive growth assays used to validate sgRNAs targeting top hit genes from the CRISPR-Cas9 screen. (b) Retesting in HeLa cells of selected sgRNAs targeting top hit genes from the CRISPR-Cas9 screen. Bars represent the average of two biological replicates.

Supplementary Figure 5



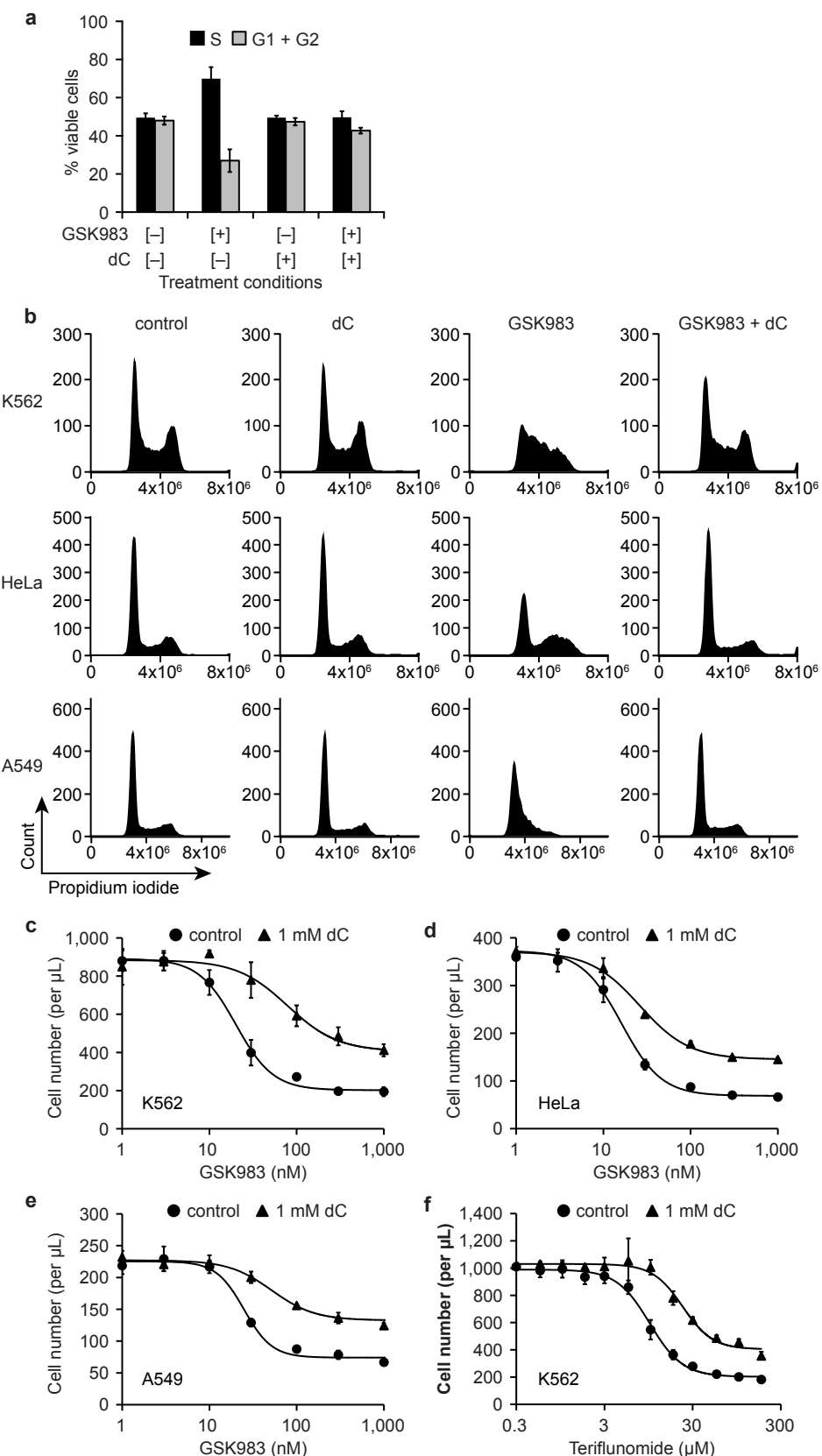
Supplementary Figure 5. **(a)** Dihydroorotic acid had no effect on GSK983-induced growth inhibition in HeLa cells. **(b)** Orotic acid reversed GSK983-induced growth inhibition in HeLa cells. For (a) and (b), viable cells were counted by flow cytometry (FSC/SSC) following 72 h treatment with 48 nM GSK983 or vehicle and the indicated concentration of (dihydro)orotic acid. Error bars represent \pm standard deviation of 4 biological replicates. Effect of **(c)** teriflunomide, **(d)** GSK983, **(e)** 6Br-pF, **(f)** 6Br-oTol, and **(g)** GSK984 on the activity of recombinant human DHODH *in vitro*. For each inhibitor, the K_i was determined with respect to the concentration of decylubiquinone (Q_d) at two different inhibitor concentrations.

Supplementary Figure 6



Supplementary Figure 6. (a) Cytidine partially reversed GSK983-induced growth inhibition in K562 cells. Viable cells were counted by flow cytometry (FSC/SSC) following 72 h treatment with 48 nM GSK983 or vehicle and the indicated concentration of cytidine. Error bars represent \pm standard deviation of 4 biological replicates. (b) Low concentrations of exogenous uridine (\leq 20 μ M) are unable to completely reverse the anti-proliferative effect of GSK983 in K562 cells. Viable cells were counted by flow cytometry (FSC/SSC) following 72 h treatment with 48 nM GSK983 or vehicle and the indicated concentration of uridine. Error bars represent \pm standard deviation of 4 biological replicates. 1 mM exogenous deoxycytidine largely reversed the anti-proliferative effect of 30 nM GSK983 in K562 cells after 3 days (c), but this effect was less pronounced after 6 days (d). Viable cells were counted by flow cytometry (FSC/SSC) following 3 day (c) or 6 day (d) treatment with the indicated concentration of GSK983 and deoxycytidine. Error bars represent \pm standard deviation of 4 biological replicates. (e) Effect of GSK983 on VEEV-GFP replication in A549 cells in the absence of exogenous pyrimidines (control, black circles), or in the presence of 1 mM uridine (blue squares), 1 mM deoxycytidine (red triangles), 1 mM dihydroorotic acid (purple diamonds), or 1 mM orotic acid (green stars). A549 cells were incubated with the indicated combination of GSK983 and pyrimidine metabolite for 24 h prior to VEEV infection. Cells were then incubated with VEEV (MOI = 20 plaque-forming units/cell) for an additional 16 h. Viral replication was measured by GFP fluorescence using flow cytometry. Error bars represent \pm standard deviation of 3 biological replicates.

Supplementary Figure 7



Supplementary Figure 7. (a) Summary of results from EdU-based cell cycle analysis shown in Fig. 3g. Error bars represent \pm standard deviation of 3 biological replicates. (b) Deoxycytidine (dC) reversed GSK983-induced S phase cell cycle arrest in K562, HeLa, and A549 cells. For all three cell lines, cells were treated with 48 nM GSK983 for 24 h, fixed in 70% EtOH, stained with propidium iodide, and analyzed by flow cytometry. For each cell line, flow cytometry plots are representative of three biological replicates. Deoxycytidine reduced GSK983 toxicity in (c) K562 cells, (d) HeLa cells, and (e) A549 cells at all growth-inhibitory doses. For (c), (d), and (e), viable cells were counted by flow cytometry (FSC/SSC) following 72 h treatment with GSK983 at the indicated concentration. Error bars represent \pm standard deviation of 4 biological replicates. (f) Deoxycytidine alleviated teriflunomide toxicity in K562 cells at all growth-inhibitory doses. Viable cells were counted by flow cytometry (FSC/SSC) following 72 h treatment with teriflunomide at the indicated concentration. Error bars represent \pm standard deviation of 4 biological replicates.

Supplementary Results

Supplementary Dataset 1. Complete gene rankings from the genome-wide shRNA screen (Microsoft Excel file available online).

Supplementary Dataset 2. Complete gene rankings from the genome-wide CRISPR-Cas9 screen (Microsoft Excel file available online).

Supplementary Table 1. Results of GO analysis (top 50 hits from the shRNA screen).

GO Category	p-value
quinone biosynthetic process	0.000560487
pyrimidine nucleoside monophosphate biosynthetic process	0.000560487
ubiquinone biosynthetic process	0.000560487
pyrimidine ribonucleoside monophosphate biosynthetic process	0.000560487
UMP metabolic process	0.000560487
ubiquinone metabolic process	0.000560487
UMP biosynthetic process	0.000560487
pyrimidine ribonucleoside monophosphate metabolic process	0.000560487
pyrimidine nucleoside monophosphate metabolic process	0.000603765
isoprenoid biosynthetic process	0.002040748
ketone biosynthetic process	0.002375797
pyrimidine ribonucleoside biosynthetic process	0.002375797
pyrimidine ribonucleotide biosynthetic process	0.002431869
quinone metabolic process	0.002564597
pyrimidine ribonucleotide metabolic process	0.002564597
pyrimidine nucleotide biosynthetic process	0.003433603
pyrimidine nucleoside biosynthetic process	0.003803045
pyrimidine ribonucleoside metabolic process	0.00418987
pyrimidine-containing compound biosynthetic process	0.005278701
pyrimidine nucleotide metabolic process	0.007333439

Supplementary Table 2. Results of GO analysis (top 50 hits from the CRISPR-Cas9 screen).

GO Category	p-value
ubiquinone metabolic process	6.32667 x 10 ⁻⁹
ubiquinone biosynthetic process	1.51045 x 10 ⁻⁷
quinone metabolic process	1.51045 x 10 ⁻⁷
cellular ketone metabolic process	1.51045 x 10 ⁻⁷
quinone biosynthetic process	1.88033 x 10 ⁻⁷
oxidoreduction coenzyme metabolic process	1.88033 x 10 ⁻⁷
coenzyme biosynthetic process	2.31975 x 10 ⁻⁶
ketone biosynthetic process	2.71449 x 10 ⁻⁶
coenzyme metabolic process	9.20268 x 10 ⁻⁶
cofactor biosynthetic process	9.20268 x 10 ⁻⁶
cofactor metabolic process	5.80963 x 10 ⁻⁵
protein tetramerization	0.000510309
isoprenoid biosynthetic process	0.003560433

Supplementary Table 3. shRNA-encoding constructs used in individual retests.

shRNA	Gene Targeted	Strand	Sequence
DHODH_1	DHODH	top	CGCCGTGGACGGACTTTATAAGTAGTGAAGCT TCAGATGTACTTATAAAAGTCCGTCCACGGCT
		bottom	AGCCGTGGACGGACTTTATAAGTACATCTGAA GCTTCACTACTTATAAAAGTCCGTCCACGGCG
DHODH_2	DHODH	top	CCCAGGGATTATCAACTCAAACACTAGTGAAGCT TCAGATGTAGTTGAGTTGATAAATCCCGGA
		bottom	TCCAGGGATTATCAACTCAAACACTACATCTGAA GCTTCACTAGTTGAGTTGATAAATCCCGGG
DHODH_3	DHODH	top	ATCTTGCAAGGACATTGAATATTAGTGAAGCT TCAGATGTAATATTCAATGTCCTTGCAAGAC
		bottom	GTCTTGCAAGGACATTGAATATTACATCTGAA GCTTCACTAATATTCAATGTCCTTGCAAGAT
DHODH_4	DHODH	top	AAAGTGTGACTCCAAAACCTCATAGTGAAGCT TCAGATGTATGAGGTTTGGAGTCACACTTC
		bottom	GAAAGTGTGACTCCAAAACCTCATACATCTGAA GCTTCACTATGAGGTTTGGAGTCACACTTT
DHODH_6	DHODH	top	AGAAGAACAAAGACCTCAGTGGATAGTGAAGCT TCAGATGTATCCACTGAGGTCTTGTCTTCC
		bottom	GGAAGAACAAAGACCTCAGTGGATACATCTGAA GCTTCACTATCCACTGAGGTCTTGTCTTCT
DHODH_7	DHODH	top	CTGCAAGGACATTGAATATTAGTAGTGAAGCT TCAGATGTACTAATATTCAATGTCCTTGCAA
		bottom	TTGCAAGGACATTGAATATTAGTACATCTGAA GCTTCACTACTAATATTCAATGTCCTTGAG
CMPK1_3	CMPK1	top	AAGAGGGGAAAGAGTAGTGGTATAGTGAAGCT TCAGATGTATACCACTACTCTTCCCTCTC
		bottom	GAGAGGGGAAAGAGTAGTGGTATACATCTGAA GCTTCACTATACCACTACTCTTCCCTCTT
CMPK1_4	CMPK1	top	AGCTGCCAATGCTCAGAAGAATTAGTGAAGCT TCAGATGTATTCTTCTGAGCATTGGCAGCC
		bottom	GGCTGCCAATGCTCAGAAGAATTACATCTGAA GCTTCACTAATTCTTCTGAGCATTGGCAGCT
CMPK1_5	CMPK1	top	ATTGCACAATGTGTTGGTAAATAGTGAAGCT TCAGATGTATTACCAACACATTGTGCAAG
		bottom	CTTGCACAATGTGTTGGTAAATACATCTGAA GCTTCACTATTACCAACACATTGTGCAAT
CMPK1_6	CMPK1	top	CCCGGTATATATCCCTCTAGTATAGTGAAGCT TCAGATGTATACTAGAGGGATATACGCGT
		bottom	ACCGGTATATATCCCTCTAGTATACATCTGAA GCTTCACTATACTAGAGGGATATACGCGG

shRNA	Gene Targeted	Strand	Sequence
PDSS1_1	PDSS1	top	ATCTCAGATAACCCTATATTAATTAGTGAAGCT TCAGATGTAATTAATATAGGGTATCTGAGAC
		bottom	GTCTCAGATAACCCTATATTAATTACATCTGAA GCTTCACTAATTAATATAGGGTATCTGAGAT
PDSS1_2	PDSS1	top	AAAGAGGAAAACACACAGTTAATAGTGAAGCT TCAGATGTATTAACTGTGTGTTTCCTCTTC
		bottom	GAAGAGGAAAACACACAGTTAATACATCTGAA GCTTCACTATTAACTGTGTGTTTCCTCTTT
PDSS1_4	PDSS1	top	AAATAGCTTTCAGCTAATAGATAGTGAAGCT TCAGATGTATCTATTAGCTGAAAAGCTATT
		bottom	GAATAGCTTTCAGCTAATAGATACATCTGAA GCTTCACTATCTATTAGCTGAAAAGCTATT
PDSS2_5	PDSS2	top	ATCACTGAAATTGGCTTAATTATAGTGAAGCT TCAGATGTATAATTAGCCAATTTCAGTGAC
		bottom	GTCACTGAAATTGGCTTAATTATACATCTGAA GCTTCACTATAATTAGCCAATTTCAGTGAT
PDSS2_7	PDSS2	top	AAGAGATCACGGAGCTAATTCTAGTAGTGAAGCT TCAGATGTATGAATTAGCTCCGTGATCTCTG
		bottom	CAGAGATCACGGAGCTAATTCTACATCTGAA GCTTCACTATGAATTAGCTCCGTGATCTCTT
PDSS2_8	PDSS2	top	CGGAGACTTCTCTAGCAAATTAGTGAAGCT TCAGATGTAATTGCTAGAAGAAAGTCTCCA
		bottom	TGGAGACTTCTCTAGCAAATTACATCTGAA GCTTCACTAATTGCTAGAAGAAAGTCTCCG
COQ10B_9	COQ10B	top	CTCAGACTATTTGTAACTTATTAGTGAAGCT TCAGATGTAATAAGTTACAAATAGTCTGAA
		bottom	TTCAGACTATTTGTAACTTATTACATCTGAA GCTTCACTAAATAAGTTACAAATAGTCTGAG
COQ10B_11	COQ10B	top	ACACGAACCTTCTCAAAATCATAGTGAAGCT TCAGATGTATGATTTGAAGAAAGTTCTCGTGC
		bottom	GCACGAACCTTCTCAAAATCATACATCTGAA GCTTCACTATGATTTGAAGAAAGTTCTCGTGT
COQ10B_12	COQ10B	top	CGAGCAGAACTCTTCCACTACATAGTGAAGCT TCAGATGTATGTAGTGGAAAGAGTTCTGCTCA
		bottom	TGAGCAGAACTCTTCCACTACATACATCTGAA GCTTCACTATGTAGTGGAAAGAGTTCTGCTCG
COQ2_2	COQ2	top	CAGCCTTGGGCTTGACATTAAATAGTGAAGCT TCAGATGTTAAATGTCAAGCCCCAAGGCTA
		bottom	TAGCCTTGGGCTTGACATTAAATACATCTGAA GCTTCACTATTAAATGTCAAGCCCCAAGGCTG

shRNA	Gene Targeted	Strand	Sequence
COQ2_3	COQ2	top	CCCTGAGGATTGTTGGAATAAAATAGTGAAGCT TCAGATGTATTATTCCAACAATCCTCAGGT
		bottom	ACCTGAGGATTGTTGGAATAAAATACATCTGAA GCTTCACTATTATTCCAACAATCCTCAGGG
COQ2_4	COQ2	top	ATGGGACCAGGACTATGATAAAATAGTGAAGCT TCAGATGTATTATCATAGTCCTGGTCCCAC
		bottom	GTGGGACCAGGACTATGATAAAATACATCTGAA GCTTCACTATTATCATAGTCCTGGTCCCAT
NegCtrl_1	none	top	AACCGGCTACTAGGTGATTAAGTAGTGAAGCT TCAGATGTACTTAATCACCTAGTAGCCGGTC
		bottom	GACCGGCTACTAGGTGATTAAGTACATCTGAA GCTTCACTACTTAATCACCTAGTAGCCGGTT
NegCtrl_2	none	top	AACTTACTAACCTCGACATCATTAGTGAAGCT TCAGATGTAATGATGTCGAAGTTAGTAAGTG
		bottom	CACTTACTAACCTCGACATCATTACATCTGAA GCTTCACTAATGATGTCGAAGTTAGTAAGTT
NegCtrl_3	none	top	AGCACTCGCATTGGAGTCAACTAGTGAAGCT TCAGATGTAGTTGACTCCGAATGCGAGTGCG
		bottom	CGCACTCGCATTGGAGTCAACTACATCTGAA GCTTCACTAGTTGACTCCGAATGCGAGTGCT
NegCtrl_4	none	top	ACGAAATTAGTTCTGGTCAATTAGTGAAGCT TCAGATGTAATTGACCAGGAACTAATTCGC
		bottom	GCGAAATTAGTTCTGGTCAATTACATCTGAA GCTTCACTAATTGACCAGGAACTAATTCGT
NegCtrl_5	none	top	CTCTCCACGACTGATATGGTAATAGTGAAGCT TCAGATGTATTACCATATCAGTCGTGGAGAA
		bottom	TTCTCCACGACTGATATGGTAATACATCTGAA GCTTCACTATTACCATATCAGTCGTGGAGAG

Supplementary Table 4. sgRNA-encoding constructs used in individual retests.

sgRNA	Gene Targeted	Strand	Sequence
NPRL2_1sg	NPRL2	top	GATAGGTGATCTTGGTCCCAGCGT
		bottom	ACGCTGGGACCCAAGATCACCTATC
NPRL2_2sg	NPRL2	top	GCTGAAGAATATGCATTGATG
		bottom	CATCGAATGCATATTCTTCAGC
DEPDC5_1sg	DEPDC5	top	GTCATCCACAAGAAGGGCTTG
		bottom	CAAAGCCCTTCTTGTGGATGAC
DEPDC5_2sg	DEPDC5	top	GTCATCCACAAGAAGGGCTT
		bottom	AAGCCCTTCTTGTGGATGAC
COQ9_1sg	COQ9	top	GGCGGCGGTATCTGGTGCCT
		bottom	AGCGCACCAAGATAACGCCGCC
COQ9_2sg	COQ9	top	GCGGTATCTGGTGCCTGGCC
		bottom	GGCCAAGCGCACCAAGATAACCGC
COQ10B_1sg	COQ10B	top	GACTGGTCATACGGCCTTGAGA
		bottom	TCTCAAGGCCGTATGACCAGTC
COQ10B_2sg	COQ10B	top	GGCCTTGAGAAGGGTAGTCTC
		bottom	GAGACTACCCTCTCAAGGCC
GFP_1sg	GFP	top	GACCAGGATGGGCACCAACCC
		bottom	GGGTGGTGCCCCATCCTGGTC

Supplementary Dataset 1. Complete gene rankings from the genome-wide shRNA screen (Microsoft Excel file available online).

Supplementary Dataset 2. Complete gene rankings from the genome-wide CRISPR-Cas9 screen (Microsoft Excel file available online).